Orthonormal (Fourier and Walsh) Models of Time-Varying Evoked Potentials in Neurological Injury

Nitish V. Thakor, *Senior Member, IEEE*, Xin-rong Guo, Christopher A. Vaz, Pablo Laguna, *Member, IEEE*, Raimon Jane, Pere Caminal, *Member, IEEE*, H. Rix, *Member, IEEE*, and Daniel F. Hanley

***Abstract*—Estimation of time-varying changes in evoked potentials (EP's) has important applications, such as monitoring high-risk neurosurgical procedures. We test the hypothesis that injury related changes in EP signals may be modeled by orthonormal basis functions. We evaluate two models of time-varying EP signals: the Fourier series model (FSM) and the Walsh function model (WFM). We estimate the Fourier and Walsh coefficients with the aid of an adaptive least-mean-squares technique. Results from computer simulations illustrate how selection of model order and of the adaptation rate of the estimator affect the signal-to-noise ratio (SNR). The FSM results in a somewhat higher steady-state SNR than does the WFM; however, the WFM is less computationally complex than is the FSM. We apply these two orthonormal functions to evaluate transient response to hypoxic hypoxia in anesthetized cats. Trends of the first five frequencies (Fourier) and sequencies (Walsh) show that the lower frequencies and sequencies may be sensitive indicators of hypoxic neurological injury.**

I. Introduction

RECENTLY, it has become apparent that EP's may be monitored to capture transient or time-varying events in the brain. For example, in neurosurgical procedures the time-course of EP signals may be an important indicator of the patient's neurological function [1], [2]. Sudden transients or unexpected time-varying changes may indicate neurological dysfunction. New signal processing techniques that serve this problem are required. Our efforts are directed toward developing signal processing techniques both for estimating time-varying changes in noisy EP signals and for understanding the diagnostic significance of these changes [3]–[5].

In neurological monitoring, because the EP signals are buried in significant (typically 0 to -15 dB) noise, the first aim of any signal processing method is the enhancement of the signal-to-noise ratio (SNR). A great deal of research has been done to identify underlying EP signals from noise [6]. Ensemble averaging is usually employed to enhance the SNR. However, during the course of neurosurgical procedures the signal may be time-varying. For such an application, a modification of the traditional procedure of ensemble averaging is necessary. In a moving window averaging scheme, for example, a specific number of sweeps may be averaged at a time. Then, successively, a new sweep is added and the oldest one discarded. Alternatively, in an exponentially-weighted averaging scheme, older sweeps are weighted less (by an exponential scale). This technique requires us to select *a priori* a weighting (or forgetting) factor that controls the speed of dynamic adaptation. Neither method constructs a model of the signal that allows interpretation of the changes resulting from injury.

We have observed that the EP signals undergo morphological changes characteristic of physiological or pathological injury [7]. This observation made apparent to us the need to construct models of the EP signal with a few parameters and to utilize these parameters for diagnostic purposes. While others, for example Norcia *et al.* [8], have analyzed time-domain as well as spectral content of the EP signal, their methods are not applicable to time-varying EP signals. Sgro *et al.* [9] have suggested a two-dimensional filter that may be suitable for time-varying EP signals, but it is not suitable for an on-line analysis since it requires acquisition of the complete ensemble before filtering can be carried out. Previously we suggested an adaptive filtering scheme, one that enhances the SNR and at the same time adapts to time-varying changes in the signal [3]. We also developed the theory behind an adaptive Fourier linear combiner [4]. Here, we propose that time-varying EP signals be modeled by two orthonormal basis functions, Fourier and Walsh. We employ an adaptive least-mean-squares (LMS) technique to estimate the model parameters and to recover the time-varying EP signal. We show that time varying changes in the model parameters may be utilized to capture incidences of neurological injury resulting from cerebral hypoxia.

II. EP Models

EP signals are obtained through repetitive stimulation of the peripheral nervous system. Successive responses should be similar. However, during the course of a complete monitoring procedure time-varying changes may be expected to occur. Typically, only the amplitudes and latencies of EP signals are recorded. A small change in amplitude or latency may or may not be diagnostically significant. In the course of routine monitoring, amplitude may change without there being any underlying pathology; for example, movement of the patient may cause such a change. Latency is a more robust indicator

Manuscript received Oct. 15, 1990; revised July 23, 1992. This work was supported by a Grant NS24282 from the National Institutes of Health, a Presidential Young Investigator Award (to NVT) from the National Science Foundation, and NATO Collaborative Research Grant CGR 90005.

N. V. Thakor, X. Guo, and C. A. Vaz are with the Department of Biomedical Engineering, The Johns Hopkins School of Medicine, Baltimore, MD 21205.

P. Laguna, R. Jane, and P. Caminal are with the Institut de Cibernetica, Barcelona, Spain.

H. Rix is with the Universite de Nice, Nice, France.

D. F. Hanley is with the Department of Neurology, The Johns Hopkins School of Medicine, Baltimore, MD 21205.

IEEE Log Number 9206324.

of pathological events, but its actual measurement (done by detecting peaks and valleys in the EP signals) is prone to errors. To avoid such errors, we propose modeling EP signals by orthonormal basis functions [10]. In such a procedure, the coefficients of the basis functions themselves may be used to detect time-varying changes. In the following, we define two orthonormal basis functions, Fourier and Walsh.

If $d(t)$ is a piece-wise continuous signal whose power within a time interval $(t_0, t_0 + T)$ is finite, then there exists a model

$$d'(t) = \sum_{m=1}^{M} c_m x_m(t) \tag{1}$$

such that

$$\int_{t_0}^{t_0+T} |d(t) - d'(t)|^2 < \epsilon$$

where ϵ can be arbitrarily small (but greater than 0), c_m is the mth coefficient of the series, M is the number of coefficients, and x_m is a real-valued function that has the following property:

$$\int_{t_0}^{t_0+T} x_m(t)\, x_n(t)\, dt = \begin{cases} \text{constant if} & \text{if } m = n \\ 0 & \text{if } m \neq n. \end{cases} \tag{2}$$

A Fourier series model (FSM) of the signal, as well as a Walsh function model (WFM), satisfies this definition. The FSM represents the signal in the form of Sine and Cosine functions, and the WFM represents the signal in the form of Cal and Sal functions. We will later utilize one property of the orthonormal representation (namely, that the signal of interest can be reconstructed with a linear combination of these functions) to recover the EP waveform. The EP signal is assumed to be quasiperiodic. That is, the waveform repeats following each successive stimulus, and the intervening signal beyond the short latency EP signals is discarded from analysis. The duration of the waveform of interest, or its period, is fixed (40 ms, or 128 samples, for the examples presented in this paper). However, the EP waveform, but not its period, may vary with time.

An FSM of an EP waveform at time k is obtained for a truncated series. Assume that the dc component is removed by filtering.

$$d'_k = \sum_{m=-M/2}^{M/2} c_m \exp(jm\omega_0 kT) \qquad k = 1, \cdots, N \tag{3a}$$

where T is the sampling interval, ω_0 is the fundamental frequency, $k = 1, \cdots, N$ are the samples in $d'_k, m\omega_0$ is the normalized frequency or the mth harmonic, and c_m are the complex coefficients. Assuming that the dc component is removed by filtering and d'_k is real, then (3a) can be expressed as

$$d'_k = \sum_{m=1}^{M/2} [a_m \operatorname{Cos}(m\omega_0 kT) + b_m \operatorname{Sin}(m\omega_0 kT)] \qquad k = 1, \cdots, N \tag{3b}$$

a_m, b_m are the mth Fourier coefficients, and the model order, by definition, is M. We choose the order M so that the truncated series represents more than 95% of the signal power. The higher harmonics are assumed to contain too little power or represent temporal features that hold little diagnostic information.

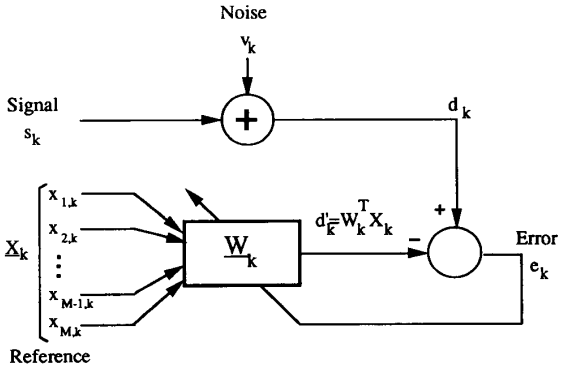

Fig. 1. Schematic of the adaptive estimator. The reference input $\boldsymbol{X}_k$ at time k represents an orthogonal set of functions $x_1, \cdots x_M$ [Fourier or Walsh; (5)]. The adaptive estimator adjusts the weights $\boldsymbol{W}_k$ (the respective coefficients) so that the MSE between the observed signal d_k at time k and the estimated signal d'_k is minimized. The LMS algorithm is employed for adaptation.

Analogous to the FSM is the representation of EP signals by a Walsh function model (WFM). The EP waveform at time k (again assuming dc coupled signals and a truncated series) is

$$\begin{aligned} d'_k &= \sum_{m=1}^{M/2} c_m \operatorname{Wal}(m, k, T) \\ &= \sum_{m=1}^{M/2} [a_m \operatorname{Cal}(m, k, T) + b_m \operatorname{Sal}(m, k, T)] \\ &\qquad k = 1, \cdots, N \end{aligned} \tag{4}$$

where $\operatorname{Wal}(m, k, T)$ is the mth Walsh function at time k. The index m defines the sequency of the Walsh function (analogous to normalized frequency for Fourier series) and M is the model order. The Cal and Sal functions take the place of the Cos and Sin functions and take advantage of computational simplicity, given that their values are 1 or 0 [10].

III. Estimation

In this section we present the algorithms to estimate the model parameters, that is, to estimate the time-varying values of the Fourier or the Walsh coefficients. The EP signal is modeled as a quasiperiodic, time-varying Fourier series or Walsh sequence. The duration, or the period, of the EP signal is fixed; but its frequency or sequency components may show unexpected variations as a result of neurological injury. The background EEG, along with environmental interference, usually adds considerable noise. For the purpose of analysis, this noise may be considered to be additive and statistically uncorrelated with the signal [6]. Hence, we employ an adaptive estimation approach that eliminates uncorrelated noise by minimizing the mean-squared error (MSE) between the noisy signal and the signal model.

Fig. 1 shows a schematic of this adaptive estimator. The primary input to the estimator at the Ath sweep is the noisy EP signal:

$$d_k = s_k + v_k \qquad k = (A-1)N+1, \cdots, AN$$

where k is the sample at time k, d_k is the observed signal, s_k is the underlying true signal, v_k is the noise added to this signal, A is the sweep number, and N is the number of samples/sweep. The reference input to the estimator are the Sin and the Cos or the Sal and the Cal functions. The signal model is constructed from a linear combination of these functions. The reference vector $\boldsymbol{X}_k$ is defined as

$$\begin{aligned}
\boldsymbol{X}_k &= [x_{1,k}, x_{2,k}, \cdots x_{M,k}]^T, \text{ where} \\
\text{FSM}: x_{r,k} &= \text{Sin}\{r\omega_0 T(k-(A-1)N)\} \\
&= \text{Sin}(r\omega_0 Tk) \quad \text{for } r = 1, 2, \cdots M/2; \\
\text{and } x_{r,k} &= \text{Cos}\{(r-M/2)\omega_0 T(k-(A-1)N)\} \\
&= \text{Cos}((r-M/2)\omega_0 T_k) \quad \text{for } r = M/2+1, \cdots, M \\
\text{WFM}: x_{r,k} &= \text{Sal}\{r, T(k-(A-1)N)\} \\
&\quad \text{for } r = 1, 2, \cdots, M/2 \\
\text{and } x_{r,k} &= \text{Cal}\{(r-M/2), T(k-(A-1)N)\} \\
&\quad \text{for } r = M/2+1, \cdots, M.
\end{aligned} \tag{5}$$

The output d'_k of the model is generated by a linear combination of the reference inputs, each one affected by a weight w_{ik} and adapted at each iteration k.

$$d'_k = \sum_{i=1}^{M} w_{ik} x_{ik} = \boldsymbol{X}_k^T \boldsymbol{W}_k = \boldsymbol{W}_k^T \boldsymbol{X}_k \tag{6}$$

where $\boldsymbol{W}_k = [w_{1,k}, w_{2,k}, \cdots, w_{M,k}]^T$ is the weight vector that we shall show is an instantaneous estimate of the Fourier or Walsh coefficients.

The adaptive estimator minimizes the MSE between the noisy input signal y_k and the signal model d'_k by adjusting the weights w_{ik}. The error signal is $e_k = d_k - d'_k$, and the mean-squared error is MSE = $E[e_k^2]$. Widrow *et al.* [11], [12] have established that the adaptive algorithm minimizes the instantaneous squared error e_k^2. In the steady state, the optimum weight vector $\boldsymbol{W}^*$ becomes

$$\boldsymbol{W}^* = \boldsymbol{R}^{-1}\boldsymbol{P} \tag{7}$$

where $\boldsymbol{R} = E[\boldsymbol{X}_k \boldsymbol{X}_k^T]$ is the input correlation matrix and $\boldsymbol{P} = E[d_k \boldsymbol{X}_k]$ is the cross-correlation vector. In our application, given that the Cal and Sal functions are orthonormal and the Sin and Cos functions can be made orthonormal with a normalization factor of 1/2,

$$\begin{aligned}
\boldsymbol{R}_{\text{FSM}} &= (1/2)\boldsymbol{I} \text{ and } \boldsymbol{P}_{\text{FSM}} = 2[a_1, \cdots, a_{M/2}, b_1, \cdots, b_{M/2}] \\
\boldsymbol{R}_{\text{WFM}} &= \boldsymbol{I} \qquad \text{and } \boldsymbol{P}_{\text{WFM}} = [a_1, \cdots, a_{M/2}, b_1, \cdots, b_{M/2}]
\end{aligned} \tag{8}$$

and therefore

$$\boldsymbol{W}^* = [a_1, \cdots, a_{M/2}, b_1, \cdots, b_{M/2}]. \tag{9}$$

This means that the weights for the two filters defined in this section converge, in steady state, to the Fourier and Walsh coefficients for the respective models. In effect, the EP signal d_k is modeled by either Fourier or Walsh functions of order M.

The Adaptive Algorithm

Different adaptive algorithms have been proposed [12]. We use the simple but effective least mean square (LMS) algorithm [11], [12]:

$$\boldsymbol{W}_{k+1} = \boldsymbol{W}_k + 2\mu e_k \boldsymbol{X}_k. \tag{10}$$

The adaptation rate of this estimator is governed by the parameter μ. The higher the value of μ, the faster the adaptation, and vice versa. However, too high a value of μ may lead to instability. From [11] the convergence condition is

$$\begin{aligned}
&0 < \mu < 1/tr[\boldsymbol{R}] \qquad (\text{FSM}: 0 < \mu < (2/M); \\
&\qquad\qquad \text{WFM}: 0 < \mu < (1/M)).
\end{aligned} \tag{11}$$

The learning curve of the adaptive algorithm is such that the MSE decreases exponentially for each mode: $(1-\mu\lambda_1), \cdots, (1-\mu\lambda_m)$, where $\lambda_i (i = 1, \cdots, m)$ are the eigenvalues of the matrix $\boldsymbol{R}$. In our algorithm, $\lambda_i = \lambda$ leads to a uniform convergence of all the modes. The time constant for convergence to the minimum MSE is $\tau = 1/(4\mu\lambda)$. Therefore, from (8)

$$\begin{aligned}
\tau_{\text{FSM}} &= 1/2\mu \quad \text{and} \\
\tau_{\text{WFM}} &= 1/4\mu.
\end{aligned} \tag{12}$$

This result demonstrates an important advantage of selecting a set of orthonormal basis functions as reference inputs. The convergence is uniform and determined by the parameter μ only as the eigenvalues are identical. If the stability condition in (11) is met, convergence can be achieved quite rapidly.

The steady-state MSE values for the FSM and the WFM are described in the Appendix. Although the steady-state MSE is a complex function involving several parameters (including μ, model order M, and the autocorrelation matrix of the reference signal $\boldsymbol{R}$), it shows a crucial linear dependence on the parameter μ when μ is small. This result makes it clear that faster adaptation is achievd by selecting a large μ, but it is achieved at the cost of a greater steady-state MSE.

IV. Simulations

We carried out several computer simulations to compare the FSM and the WFM models, and to illustrate the performance of the adaptive estimator. These simulations examine the selection of model order, adaptation rate, transient response, and steady state performance. For the purpose of these simulations we created an EP template by ensemble averaging 1000 sweeps that were recorded during the normal control period of the experiment reported in this paper. This template was considered to be the true signal s_k. For the purpose of our simulations, we consider that the prestimulus signal constitutes background brain activity or noise. This prestimulus noise v_k was added to the EP template to generate a noisy sweep $d'_k = s_k + v_k$. The noise level was scaled to alter the SNR, and several thousand noisy sweeps were generated in this manner.

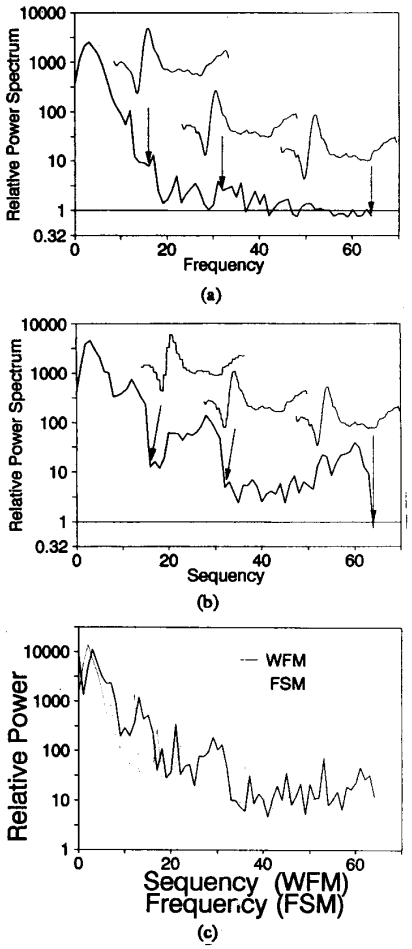

Fig. 2. Relative power spectra $(a_m^2 + b_m^2)$ for EP signals and pre-stimulus noise. (a) Fourier model, (b) Walsh model. The insets show waveforms produced when reconstruction is done using frequency/sequency terms up to 16, 32, and 64 (model orders 32, 64, and 128, respectively). The spectra for $A = 200$ sweeps are averaged. (c) Relative power versus frequency (Fourier) or sequency (Walsh) for prestimulus noise.

Model Order

It is important to select a proper model order to represent the signal accurately. Truncation of either the Fourier or the Walsh series produces a distortion of the time domain signal, leading to possible inadequate representation of the fine features of the waveform. Choice of an appropriate model order becomes apparent from the discrete Fourier transform and the Walsh transform. Fig. 2 plots the relative power, defined as $(a_m^2 + b_m^2)$, at various frequencies (harmonics), in the case of Fourier, or sequencies, in the case of Walsh. The waveforms in the inset show that truncation of the Fourier series results in a lowpass filtering or smoothing effect in the reconstructed signal. Nevertheless, even with a smaller order, reconstruction retains the significant features of the EP signal [see inset, Fig. 2(a)]. A high order Walsh model also adequately reconstructs the signal, but at lower orders the Walsh function results in a fairly jagged waveform that may not be clinically acceptable [see inset, Fig. 2(b)]. The appearance can be cosmetically improved, if necessary, by smoothing the reconstructed waveform. In practice, we select a model order high enough to include more than 95% of the signal energy.

TABLE I
COMPARISON OF THE FSM AND THE WFM (M: MODEL ORDER ; $k = 1 \cdots N$, NO. SAMPLES /SWEEP)

	WFM	FSM
Memory (bytes)	(M/8)k	(M/2)k
Calculations: Multiplications	1	2M+1
Calculations: Add/subtract	2M	2M
Steady-state % error: $\left\{\sum_{k=1}^{N}(s_k - d'_k)^2 / \sum_{k=1}^{N}(s_k)^2\right\}$ x100		
M=32	5.6%	2.0%
M=64	2.7%	1.8%
M=128	1.7%	1.7%

Table I compares the memory and computing requirements for several models. We also show in Table I the steady-state error (the normalized squared value of the difference between each sample of the known template s_k and the filter output d'_k at all frequencies or sequencies). While the errors are comparable at $M = 128$ for the WFM and FSM, at model orders below $M = 32$ the error is noticeably greater for the WFM.

Next, we evaluated the effect of model order selection and the adaptation parameter values for the two models. Fig. 2(c) shows that the power spectrum of noise overlaps the Fourier and the Walsh spectra of the signal in Fig. 2(a) and (b), although not completely. The insets in Fig. 2(a) and (b) illustrate the EP template reconstructed using 16, 32, and 64 frequencies or sequencies for the FSM and WFM, respectively. As expected, the template reconstruction improves as the number of frequencies or sequencies used in the reconstruction is increased.

Fig. 3 plots the SNR at successive sweeps for the two models. The SNR is defined as

$$\text{SNR} = \left\{\sum_{k=1}^{N} s_k^2\right\} \Big/ \left\{\sum_{k=1}^{N}(s_k - d'_k)^2\right\}. \qquad (13)$$

In the steady state, that is after all the weights have converged, there is some residual estimation error. The steady state error is caused by truncation, which results from the selection of the model order M, and misadjustment, which results from the LMS algorithm. Increased steady state error due to truncation at smaller model orders is apparent in Fig. 3. Truncation error is noticeable for the WFM at model orders below $M = 32$. Truncation error can be minimized by selecting a higher model order, but at the cost of increased computations and memory requirements (Table I). Also note that a larger model order results in a larger misadjustment error.

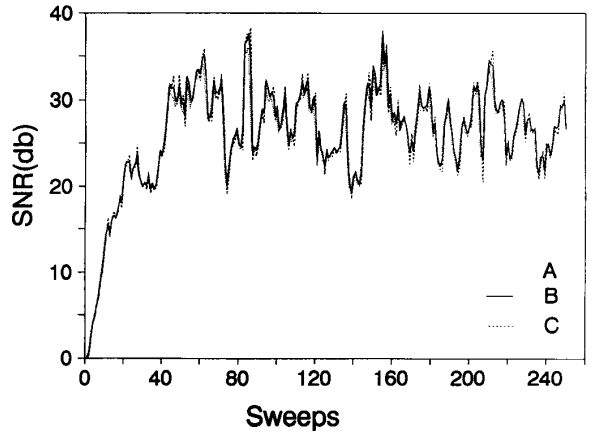

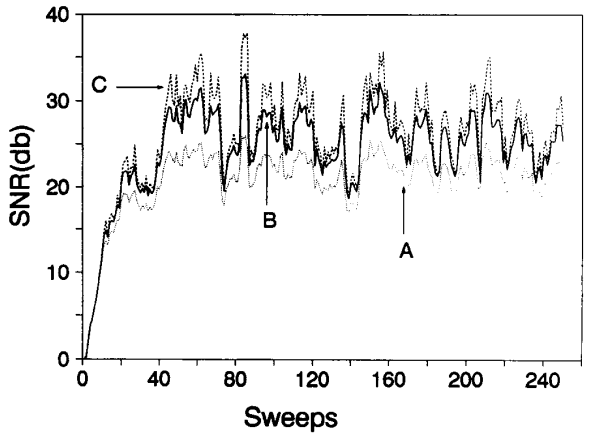

Fig. 3. Estimator response for various model orders. (a) FSM estimator. (b) WFM estimator. For comparison, equivalent model orders (A: $M = 32, B$: $M = 64$, and C: $M = 128$) and convergence rates [$\mu = 0.0003$ (WFM) and 0.0006 (FSM)] are used.

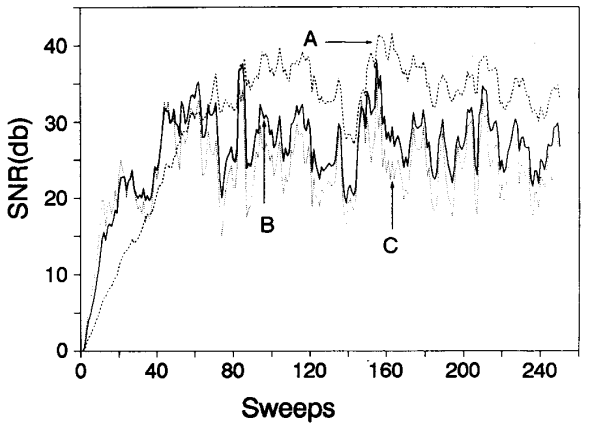

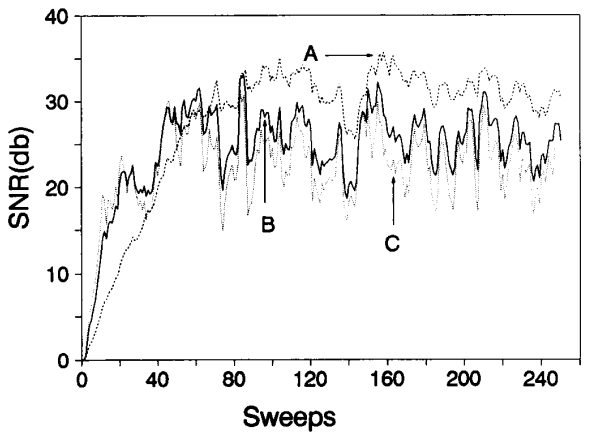

Fig. 4. Estimator response for various adaptation parameter values. (a) FSM estimator. (b) WFM estimator. In general, a larger value of μ results in faster adaptation but also greater steady-state misadjustment error (or lower SNR). [$M = 64, A$: $\mu = 0.0003, B$: $\mu = 0.0007, C$: $\mu = 0.001$ (WFM); and A: 0.0006, B: 0.0014, C: 0.002 (FSM)].

Adaptation

In order to study the adaptation properties of the algorithm, we analyzed the database constructed previously. We employed the adaptive LMS algorithm, where the parameter μ governs the adaptation rate [see (12)]. Note that the adaptation occurs at each sample, and therefore, a μ value in the range of 0.0001 ($\tau = 5000$) achieves adaptation in about 50 sweeps for an EP waveform with 128 sample points per sweep. The higher the value of μ, the faster the adaptation, and this allows us to track faster EP transients (Fig. 4). Unfortunately, a larger value of μ also results in a greater steady-state misadjustment error [12]. This is actually quite apparent with the WFM [Fig. 4(b)]. To achieve a high steady-state SNR, it is important to select a smaller value of μ (although we may sacrifice some transient response). Equation (A.2) in the Appendix suggests that at higher levels of noise in the EP signals, the MSE would be reduced by selecting smaller values of μ.

Transient Response

A significant advantage of the adaptive estimator is that we can follow time-varying changes in the EP waveform. For example, in Fig. 5 we abruptly alter the EP waveform. As before, the simulation data contain experimentally recorded EEG noise added to the known EP signal. During the first 100 sweeps, both the FSM and the WFM estimators (with comparable model orders and μ values) adapt until they reach a steady state. After the abrupt change in the signal, there is an initial sharp drop in the SNR. While both the estimators reach a steady-state SNR in about 60 sweeps (Fig. 5), the FSM estimator produces a slightly higher steady-state SNR.

V. Experimental Studies

We conducted an experimental study to evaluate the FSM and WFM models of EP signals under normal and hypoxic injury conditions. We carefully followed the transient response of the FSM and the WFM estimators throughout the course of brain injury and recovery. Our aim was to determine whether the two estimators captured the incidence of hypoxia and

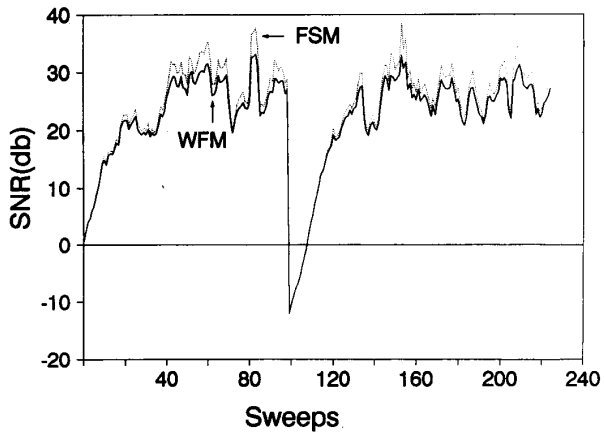

Fig. 5. Transient response of the FSM and the WFM estimators. The EP signal in the inset is abruptly changed to a new one at the 100th sweep. Equivalent model orders and convergence times are used for comparison. (μ = 0.0007 (WFM) and 0.0014 (FSM); M = 64).

whether changes in the model parameters provided any early indications of injury.

We considered acute cerebral hypoxia as a model of brain injury. Anesthetized cats were made hypoxic in order to alter the response of their nervous system. The experimental protocol was similar to the one described by McPherson *et al.* [13]. The animals were anesthetized with ketamine and acepromazine given intramuscularly (50 mg/kg/h and 1.1 mg/kg/h, respectively). Anesthesia was maintained with nitrous oxide and intravenous fentanyl (21.5 μg/h). After the scalp, skin, and musculature were dissected, a ball-shaped silver electrode with shielded cable was placed in a hole approximately 1 cm lateral to the midline and just prior to the coronal suture. A reference electrode was placed in a hole drilled in the frontal bone, and stimulating electrodes were placed percutaneously on the volar surface of the contralateral leg. The anesthetized cat initially breathed normal air, but after a period of adaptation, the cat breathed a hypoxic gas mixture (8% O_2). After the animal was anesthetized, electrical stimuli of 0.2 ms duration were delivered at supra-threshold strength (typically 20 mA) at the rate of 5.9/s. A commercial amplifier (Nicolet Med80) acquired raw (unaveraged) EP sweeps. Each sweep, which comprised 128 samples, was digitized at the rate of 3200 samples/s (using an ISC-16 data-acquisition system, RC Electronics). The data were acquired and analyzed on an IBM-compatible, Intel 386 microprocessor-based personal computer. Detailed experimental results are described by Vaz [7]. The data in Fig. 6 show a transient loss in EP signal amplitude, with the decline taking place over a span of about 4000 sweeps. When the cat was returned to normoxic air its recovery was surprisingly quite rapid, taking place in less than 1000 sweeps. This result suggests that the proposed adaptive algorithm is sensitive to transient changes resulting from acute injury to the brain.

An inspection of the EP waveforms in the inset of Fig. 6(a) and (b) reveals that besides changes in signal amplitude noticeable changes occur in signal shape as well. We plotted the time-varying changes in the mean amplitudes for the first five

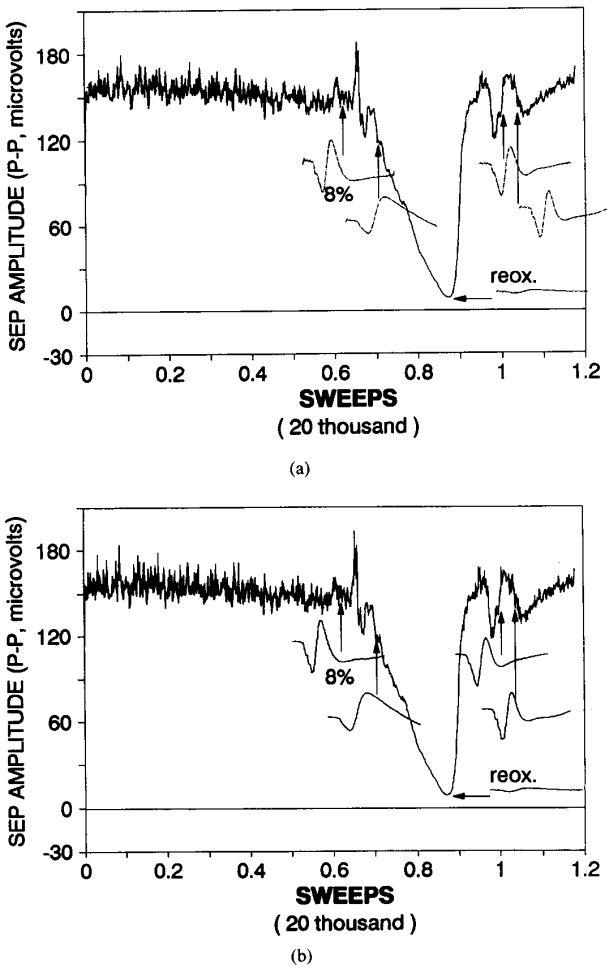

Fig. 6. Transient amplitude response of somatosensory EP to hypoxic hypoxia (8% inspired O_2) and reoxygenation (reox.) in an anesthetized cat. (a) FSM estimator, and (b) WFM estimator. The inset shows waveforms estimated using the adaptive algorithms during control, 8% O_2, at the time of recovery with 100% O_2, and following full recovery [y axis: amplitude of the somatosensory EP signal peak; x axis: number of sweeps with the scale multiplied by 20 000; μ = 0.0007 (WFM) and 0.0014 (FSM)].

frequencies and sequences (FSM and WFM, respectively) at each successive sweep throughout the course of the experiment [Fig. 7(a) and (b)]. Quite surprisingly, the relative distribution of various frequencies or sequencies shows distinct trends during hypoxic injury and during recovery. Specifically, the first frequency/sequency appears to respond strongly to cerebral hypoxia in the early stages. The lower frequencies (1 to 3) also appear to be the earliest to recover after reoxygenation. This result suggests that time-varying changes in the signal model can be used to examine the nature of neurological injury.

VI. Discussion and Conclusions

The FSM and the WFM provide alternative ways of modeling time-varying EP signals. Since these are orthonormal basis functions, they possess some unique advantages. A relatively few basis functions suffice, and a truncated set may also be

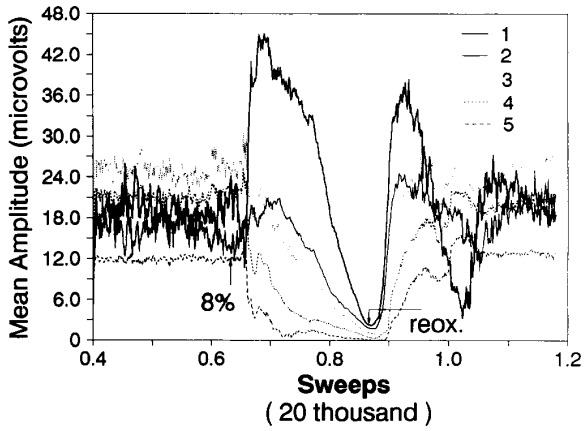

(a)

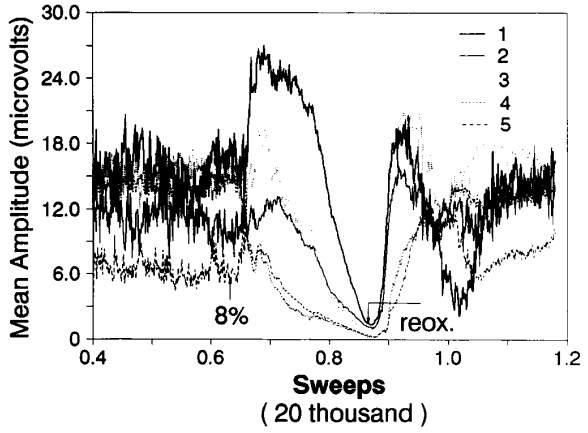

(b)

Fig. 7. Time trends of mean amplitudes for (a) the first five frequencies (FSM) and (b) the first five sequencies (WFM). Note the increased response of the first frequency/sequency during the early stages of hypoxia (8% O_2). Note also the relatively rapid recovery of the lower frequencies/sequencies (1–3) following reoxygenation (reox.). (y axis: mean amplitude; x axis: number of sweeps with the scale multiplied by 20 000; $\mu = 0.0007$ (WFM) and 0.0014 (FSM); mean amplitude is calculated as: $\sqrt{\sum_{m=1}^{M/2}(a_m^2 + b_m^2)}$, where a_m and b_m are the Fourier or the Walsh coefficients.

selected. The adaptive estimator employs the LMS algorithm, which has the advantage of computational simplicity. Also, since we use an orthonormal reference set, there is no eigenvalue spread and, as a result, convergence of all the model coefficients is uniform; hence, no distortion occurs. In general, the FSM requires a smaller model order and results in a higher steady-state SNR. A high model order is desirable with the WFM to achieve adequate signal representation. The jagged, step-like appearance of the Walsh estimated waveform may not be aesthetically acceptable. However, the WFM estimator requires fewer calculations and smaller memory capacity and, therefore, may be preferred to real-time applications (Table I). For the two applications in this paper, both the FSM and the WFM estimators produce similar results. The benefit of the FSM is a somewhat higher steady-state SNR, an aesthetically pleasing reconstruction of the EP waveform, and a more traditional frequency domain interpretation of the signal.

The primary reason to select Fourier and the Walsh basis functions is that they are orthonormal, and also that they are mathematically well understood [10]. Another convenient benefit of our selection is that the frequencies and harmonics of the Fourier series are well understood and accepted in clinical applications. Our experiments also show that the time-varying response of various frequencies/sequencies to neurologic injury occasionally differs. Therefore, an advantage of our approach is that, in the course of estimation, we build a model of the signal that may be useful for diagnostic purposes. For example, our experimental studies appear to indicate that the lower frequencies/sequencies are the more sensitive indicators of hypoxic injury [13]. Our second selection, Walsh basis, was chosen for its analogy to the Fourier basis and its significant computational simplicity (Table I). The result obtained in this paper, that the performance of the Walsh model is only marginally inferior to that of the Fourier model, is important if this algorithm is to be implemented in a real-time system. We do not now know what diagnostic or computational advantage basis functions other than Fourier and Walsh would offer.

Selection of model order may be important in some applications where subtle changes in the waveform may have to be discriminated. In this paper we truncate the model, and truncation may result in some distortion. In practice this is not a problem if the model order is high enough so that more than 95% of the signal energy is represented. Of course, a smaller model order has the advantage that fewer calculations and less data storage space are required. The model order selected affects the steady-state SNR. The higher the model order, the higher the steady-state SNR. A smaller model order results in a greater steady-state misadjustment (lower SNR), but the advantage of the smaller model order is that it requires fewer calculations. The reduced computational load may be important in real-time monitoring. An indirect benefit of EP signal modeling is data compression, that is to say, at each sweep only the model coefficients need be saved; individual sample values need not. Therefore, a smaller model order representation requires less data-storage capacity. In the current study, we do not adjust the model order dynamically (that is, sweep by sweep) because it is not clear that any improvement in SNR could be achieved whereas further signal distortion is risked. However, (A.1) and (A.2) in the Appendix do suggest the prospect of selecting an optimal model order for achieving the desired MSE. Such an algorithm would be very data-dependent.

The adaptation parameter μ governs the convergence properties of the adaptation algorithm. As the result in the Appendix shows, a complex relationship exists between the adaptation error ϵ and the adaptation rate parameter μ. A large value of μ allows the algorithm to track faster transients at the expense of a greater adaptation error. As the simulation results show, an SNR improvement of 10–20 dB with realistic, experimental, or clinical somatosensory EP recordings can be achieved for a μ value in the range of 0.001–0.0001. The steady-state SNR between 10 and 20 dB is reached in

about 100 sweeps. The SNR may vary during the actual experiments. A more advanced algorithm could dynamically alter the adaptation parameter μ to a higher value in low-noise situations. This would allow the algorithm to track more rapid transients.

The adaptive LMS algorithm employed in this paper has been shown to converge to the Wiener filter $\boldsymbol{W}^*$ [11], [12]. In the steady-state, the EP estimates are expected to converge to the optimum Wiener filter. However, when the signals are time-varying and when the signal and noise are correlated, this conclusion will not hold true. In the experiments presented here, the signals are indeed time-varying and the Wiener filtering approach is not appropriate when real-time monitoring must be carried out without a priori information. In certain situations, the noise may be correlated with the signals, such as when strong quasiperiodic alpha activity is present. In the examples presented here, in which we analyzed the somatosensory EP signals of cats under anesthesia, we did not observe enhanced alpha activity. Periodic components of the electrical interference, such as 60 and 120 Hz power line signals, will not be cancelled by the method proposed here. This electrical interference should be eliminated prior to data-acquisition by analog notch filtering, or by an adaptive 60 Hz canceller [11].

Together, these signal models of EP and the adaptive estimation algorithm serve as tools for monitoring transient and time-varying EP signals. Our experimental study reveals that the Fourier and Walsh models may be useful in examining the time course of neurological injury. Since various frequencies/sequencies respond differently to the neurological injury and to recovery, they may be used to evaluate the nature and extent of injury. Based on the experimental results presented here, we hypothesize that the lower frequencies/sequencies may be used as early indicators of the incidence of neurological injury and their recovery. Evaluation with other models of neurological injury, such as cerebral ischemia [14], may be needed to confirm whether changes in the lower frequencies/sequencies are universal indicators of brain injury. Observations made under controlled experimental situations remain to be tested in clinical environments where alterations in evoked potentials due to injury have been reported [15]. Alterations occurring due to neurological injury must also be discriminated from the effects caused by anesthetics. We did not observe changes in model parameters with one anesthetic (etomidate) [5]; however, other anesthetics [16] remain to be studied. While we have observed that the responses of the Fourier and Walsh models are similar, a more detailed examination and additional experimental studies would be needed to determine the relative clinical merit of the two models. Note, however, that Fourier and Walsh analyses of EEG signals have also produced similar results in tracking the effects of anesthesia [17].

Brain monitoring in critical care situations, such as in a neurological intensive care unit and in high-risk surgical procedures, would benefit from signal models that help identify risk to patients. In surgical situations, where the alteration in an EP signal may occur unexpectedly, such as due to occlusion of a cerebral artery [1], [2], [14], our algorithms may be expected to supply a rapid indication. For example, time trends of the changes in various frequencies/sequencies may be continuously monitored for this purpose. Real-time and on-line estimation and display would help in timely detection of trauma to the brain and may lead to quick corrective actions. The algorithms presented here, therefore, may conveniently be employed in patient-monitoring systems.

VII. Appendix

An expression for steady-state error (that is, MSE), after the statistical moments of the weight vector have converged, can be derived and used in assessing the performance of the proposed algorithm. The steady-state MSE consists of two components:

$$\xi = \epsilon + f(M), \text{where}$$

$$\epsilon = \lim_{k\to\infty} E[(s_k - d'_k)^2] \text{ is the adaptation error and}$$

$$f(M) = \sum_{i=(M/2)+1}^{N/2} (a_i^2 + b_i^2)$$

is the truncation error for model order M. (A.1)

A detailed expression is obtained following the derivative of Vaz and Thakor [4]. The analysis assumes that 1) $\mu \ll 1$, and 2) noise v_k is zero-mean, stationary, and uncorrelated with the signal, and autocovariance $R_v(i) = E[v_k v_{k+i}] = 0$ beyond a finite interval, i.e., for $i > L$. If $R_i = E[\boldsymbol{X}_i \boldsymbol{X}_i^T]$ is the autocorrelation matrix of the reference vector, M is the model order (in case of WFM, M is a power of 2, or $M = 2^n$), then, for the two models in this paper,

$$\text{FSM: } \epsilon = \mu R_v(0) M + 2\mu \sum_{i=1}^{L} (1-\mu)^i R_v(i) \sum_{j=1}^{M} \cos(j\omega_0 i)$$

$$\text{WFM: } \epsilon = \left(\frac{\mu}{1-\mu}\right) R_v(0) n + \left(\frac{\mu}{1-\mu}\right) \sum_{i=1}^{L} (1-2\mu)^j R_v(i) tr[R_i + R_{-i}]. \quad \text{(A.2)}$$

The detailed derivations are available from the authors upon request.

References

[1] B. L. Grundy, "Intraoperative monitoring of somatosensory evoked potentials," *Anesthesiol.*, vol. 58, pp. 72–87, 1983.

[2] R. W. McPherson, "Intraoperative monitoring of evoked potentials," *Prog. Neurol. Surg.*, vol. 12, pp. 146–163, 1987.

[3] N. V. Thakor, "Adaptive filtering of evoked potentials," *IEEE Trans. Biomed. Eng.*, vol. 34, pp. 6–12, 1987.

[4] C. A. Vaz and N. V. Thakor, "Adaptive Fourier estimation of time-varying evoked potentials," *IEEE Trans. Biomed. Eng.*, vol. 36, pp. 448–455, 1989.

[5] N. V. Thakor, C. A. Vaz, R. W. McPherson, and D. F. Hanley, "Fourier series modeling of time-varying evoked potentials," *J. Electroenceph. Clin. Neurophys.*, vol. 80, pp. 108–118, 1991.

[6] J. I. Aunon, C. D. McGillem, and D. G. Childers, "Signal processing in evoked potential research: averaging, principal components, modeling," in *Crit. Rev. Biomed. Eng.*, CRC Press: Cleveland, OH, vol. 5, 1981, pp. 323–367.

[7] C. A. Vaz, "Adaptive Fourier estimation of time-varying evoked potentials" *Ph.D. dissertation*, The Johns Hopkins University, Baltimore, MD, 1990.

[8] A. M. Norcia, T. Sato, P. Shinn, and J. Mertus, "Methods for the identification of evoked response components in the frequency and combined time/frequency domains," *Electroenceph. Clin. Neurophys.*, vol. 65, pp. 212–226, 1986.
[9] J. A. Sgro, R. G. Emerson, and T. A. Pedley, "Real-time reconstruction of evoked potentials using a new two-dimensional filter method," *Electroenceph. Clin. Neurophys.*, vol. 62, pp. 372–380, 1985.
[10] N. Ahmed and K. R. Rao, *Orthogonal Transforms for Digital Signal Processing*. Springer-Verlag: Berlin, 1975.
[11] B. Widrow, J. R. Glover, J. M. McCool, J. Kaunitz, C. S. Williams, R. H. Hearn, J. R. Zeidler, E. Dong, and R. C. Goodlin, "Adaptive noise canceling: principles and applications," *Proc. IEEE*, vol. 63, pp. 1692–1716, 1975.
[12] B. Widrow, S. D. Stearn, *Adaptive Signal Processing*. Prentice Hall: Englewood Cliffs, NJ, 1985.
[13] R. W. McPherson, S. Zeger, and R. J. Traystman, "Relationship of somatosensory evoked potentials and cerebral oxygen consumption during hypoxic hypoxia in dogs," *Stroke*, vol. 17, pp. 30–36, 1986.
[14] N. Matsumiya, R. C. Koehler, and R. J. Traystman, "Consistency of cerebral blood flow and evoked potential alterations with reversible focal ischemia in cats," *Stroke*, vol. 21, pp. 908–916, 1990.
[15] B. L. Grundy, R. C. Heros, A. S. Tung, and E. Doyle, "Intraoperative hypoxia detected by evoked potential monitoring," *Anesth. Analg.*, vol. 60, pp. 437–439, 1981.
[16] A. Koht, W. Schwartz, G. Schmidt, J. Schramm, and E. Watanabe, "Effects of etomidate, midazolam, and thiopental on median nerve somatosensory evoked potentials and the additive effects of fentanyl and nitrous oxide," *Anesth. Analg.*, vol. 67, pp. 435–441, 1988.
[17] R. Dzwonczyk, M. Howie, and J. S. McDonald, "A comparison between Walsh and Fourier analysis of the electroencephalogram for tracking the effects of anesthesia," *IEEE Trans. Biomed. Eng.*, vol. 31, pp. 551–556, 1984.

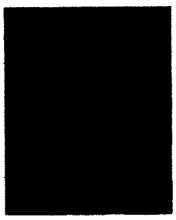

Nitish V. Thakor (S'78–M'81–SM'89) received B.Tech. degree in electrical engineering from Indian Institute of Technology, Bombay, in 1974 and the Ph.D. degree in electrical and computer engineering from the University of Wisconsin, Madison, in 1981.

He previously served on the faculty of Electrical Engineering and Computer Science of the Northwestern University, and is currently on the faculty of the Department of Biomedical Engineering at the Johns Hopkins Medical School where he teaches and conducts research in the areas of Medical Instrumentation, Signal Processing and Computer Applications. He serves on the editorial board of several journals, including the IEEE TRANSACTIONS ON BIOMEDICAL ENGINEERING and is actively developing scientific programs, tutorials, and books on the topics of Biomedical Signal Processing, Neuroengineering, and Computers in Biomedical Engineering.

Dr. Thakor is a recipient of a Research Career Development Award from the National Institutes of Health and a Presidential Young Investigator Award from the National Science Foundation.

Xin-rong Guo received the B.S. degree and M.S. degree in electrical engineering from the University of Science and Technology of China, Hefei, P. R. China in 1972 and 1981, respectively.

He was a faculty member in Electrical Engineering Department, University of Science and Technology of China, Hefei, P. R. China, from 1981 to 1989, where he was engaged in speech recognition, signal detection and processing, system analysis. From 1989 to 1991, he was a visiting scholar in the Biomedical Engineering Department, Johns Hopkins School of Medicine, Baltimore, MD, working on adaptive filtering and data compression. He is now a research staff in the Ophthalmology Department, Johns Hopkins School of Medicine, Baltimore, MD. His research interests include signal detection and processing, image processing, speech recognition and synthesis, and microcomputer application.

Christopher A. Vaz, photograph and biography not available at the time of publication.

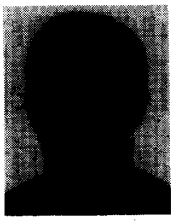

Pablo Laguna received the M.S. degree in physics and the Ph.D. degree in physical science from the Science Faculty at the University of Zaragoza, Spain, in 1985 and 1990, respectively.

He is an Associate Professor of Signal processing in the Department of Electrical Engineering and Informatics at the University of Zaragoza, Spain. From 1987 to 1992 he worked as Assistant Professor of Automatic control in the Department of Control Engineering at the Politecnic University of Catalonia (U.P.C.), Spain and as a Researcher at the Biomedical Engineering Division of the Institute of Cybernetics (U.P.C.–C.S.I.C.). His research interest is signal processing, in particular as applied to Biomedical applications.

Raimon Jane received the electrical engineering degree and the doctor engineer degree from the School of Industrial Engineering of Barcelona at the Polytechnic University of Catalonia (U.P.C.), Spain, in 1983 and 1989, respectively.

From 1984 to 1989 he worked as a Research Assistant at the Biomedical Engineering Division of the Institute of Cybernetics (U.P.C.–C.S.I.C.), where he is now a Researcher. His current research interests are digital signal processing applications to biological signals, and in particular, high resolution ECG. He currently teaches medical instrumentation and signal processing in the Master and Doctoral programs in Biomedical Engineering, at the Polytechnic University of Catalonia.

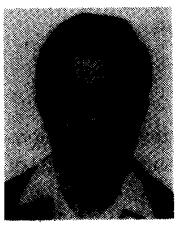

Pere Caminal (M'88) received the M.S. and Ph.D. degrees in mechanical engineering in 1974 and 1980, respectively, from the Polytechnic University of Catalonia (U.P.C.), Spain.

He is a Professor of Automatic Control in the Department of Control Engineering at the same University. He is presently the head of the Biomedical Engineering Division of the Institut of Cybernetics (U.P.C.), and director of the Master in Biomedical Engineering Degree Program at the Polytecnic University of Catalonia. His areas of interest are modeling and simulation of biological systems, and processing.

H. Rix (A'88), photograph and biography not available at the time of publication.

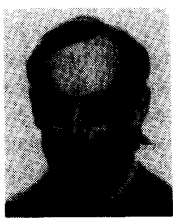

Daniel F. Hanley received the B.A. degree from Williams College, Williamstown, MA, in 1971 and the M.D. degree from Cornell University Medical College, New York, NY, in 1975. His past positions include an internship and residency in medicine at The New York Hospital in 1976 and 1977; a Kettering Research Fellow at The Sloan-Kettering Institute in New York in 1978; a neurology residency at The Johns Hopkins Hospital in 1979; followed by a research fellowship in the departments of neurology/neurosurgery and anesthesia in 1981. Upon completing his fellowships, he became assistant professor in the departments of neurology/neurosurgery and anesthesia in 1983. In 1982 he played a major role in organizing and instituting the Johns Hopkins Neurosciences Critical Care Unit of which he is the Director. He became the Director of the Neurology Residency Program of Johns Hopkins Department of Neurology in 1990 in addition to being promoted to the level of Associate Professor in the departments of neurology/neurosurgery and anesthesia. He has research interests in the physiology of acute illness including cerebral blood flow and metabolism, cranial vault mechanics, and electrophysiology in acute illness.